too unstable with respect to ligand oxidation to function effectively in this capacity.

Acknowledgment. We have benefited from discussions with Arthur J. Frank and Roger Palmans (SERI, Golden, CO) and Francois P. Rotzinger (EPFL, Lausanne, Switzerland). Funding for this research was provided by the Office of Basic Energy Sciences, U.S. Department of Energy, under Grant DE-AC-06-83ER-13111. We are grateful to them for their interest and support.

Contribution from the Department of Chemistry,
The University of North Carolina at Charlotte, Charlotte, North Carolina 28223

Multimetallic Ruthenium(II) Complexes Based on Biimidazole and Bibenzimidazole: Effect of Dianionic Bridging Ligands on Redox and Spectral Properties

D. Paul Rillema,* Ram Sahai, Philomina Matthews, A. Kirk Edwards, Randy J. Shaver, and Larry Morgan

Received May 1, 1989

The preparation and properties of ruthenium(II) complexes containing the ligands 2,2′-biimidazole ($BiImH_2$), 2,2′-bibenzimidazole ($BiBzImH_2$), and 2,2′-bipyridine (bpy) are reported. The complexes described are $[(Ru(bpy)_2)_2BiIm]^{2+}$ and the series $[Ru(bpy)_n(BiImH_2)_{3-n}]^{2+}$, $[Ru(bpy)_n(BiBzImH_2)_{3-n}]^{2+}$, and $[Ru(bpy)_n(BiBzImRu(bpy)_2)_{3-n}]^{2+}$, $n = 0$–2. The redox potential for the first $Ru^{3+/2+}$ couple shifted negatively from 1.26 to −0.26 V vs SSCE as bpy ligands were replaced by $BiImH_2$, $BiBzImH_2$, and "$BiBzImRu(bpy)_2$" ligands. The $BiBzImRu(bpy)_2$ units shifted the redox potential a factor of 3 greater than that for $BiBzImH_2$, which was attributed to greater electrostatic interaction of the dinegatively charged bridging ligands following deprotonation. The magnitude of the shift was such that the tetrametallic species was isolated as the $[Ru^{III}(BiBzImRu^{II}(bpy)_2)_3)]^{3+}$ cation. Reductions were found in the −1.5- to −1.6-V range for complexes containing bipyridine ligands, but none were observed out to −2.0 V for $[Ru(BiImH_2)_3]^{2+}$ or $[Ru(BiBzImH_2)_3]^{2+}$. The complexes absorbed energy in the visible and UV regions of the spectrum and emitted radiation, with the exception of the tetrametallic species, in the 600–800-nm region. The emission was weak, $\phi_r = 10^{-3}$–10^{-4}; the excited-state lifetimes ranged from 25 to 161 ns. Estimates of the excited-state redox potentials revealed that the excited-state species were powerful reductants, $E_{1/2}(Ru^{3+/2+*}) \sim -0.8$ V, but were weak oxidants, $E_{1/2}(Ru^{2+*/+}) \sim 0.2$ V. The $[Ru^{III}(BiBzImRu^{II}(bpy)_2)_3]^{3+}$ cation absorbed in the near-infrared region at 12.2×10^3 cm^{-1} in acetonitrile, but the absorption disappeared upon reduction to $[Ru^{II}(BiBzImRu^{II}(bpy)_2)_3]^{2+}$. The position of the absorption manifold maximum varied linearly with the static and optical dielectric constant of the solvent. The width of the absorption band was comparable to that of $[Ru^{III}(bpy)_2BiBzImH_2]^{3+}$, but its intensity was greater. The band at 12.2×10^3 cm^{-1} was attributed to overlapping LMCT and metal to metal charge transfer.

Introduction

Studies in our laboratories have centered on the design of multimetallic complexes based on bidentate bridging ligands with the ultimate goal of effecting multiple-electron-transfer events from excited-state species. Our efforts have resulted in the isolation of ruthenium/ruthenium,[1,2] ruthenium/platinum,[3-5] and ruthenium/rhenium[6] complexes. We have, for example, isolated the $[Ru(bpqRu(bpy)_2)_3]^{8+}$, $[Ru(bpqPtCl_2)_3]^{2+}$, and $[Ru(bpmRe(CO)_3Cl)_3]^{2+}$ cations as PF_6^- salts, where bpq is 2,3-bis(2-pyridyl)quinoxaline, bpm is 2,2′-bipyrimidine, and bpy is 2,2′-bipyridine. The multimetallic complexes were formed by addition of the appropriate precursor to the remote nitrogen donors on the ligands of the parent $[Ru(bpq)_3]^{2+}$ and $[Ru(bpm)_3]^{2+}$ complexes. The presence of more than one metal with these bridging ligands shifts the luminesce to the red side of the spectrum approximately 100 nm and decreases the luminescence intensity by at least 1 order of magnitude.[7] However, complexes formed from bridging ligands with a saturated alkyl linkage retained their luminescence integrity. The $[(bpy)_2Ru(Mebpy\text{-}Mebpy)PtCl_2]^{2+}$ complex, for example, where Mebpy-Mebpy is 1,2-bis(4′-methyl-2,2′-bipyridiyl-4-yl)ethane, was nearly as emissive[4] as $[(bpy)_2Ru(Mebpy\text{-}Mebpy)]^{2+}$.

In this paper, we report complexes based on a different type of bridging ligand. Biimidazole and bibenzimidazole shown in Figure 1 were used to effect bridging from one ruthenium(II) center to another and enabled us to prepare $[(Ru(bpy)_2)_2BiIm]^{2+}$ and the series $[Ru(bpy)_n(BiImH_2)_{3-n}]^{2+}$, $[Ru(bpy)_n(BiBzImH_2)_{3-n}]^{2+}$, and $[Ru(bpy)_n(BiBzImRu(bpy)_2)_{3-n}]^{2+}$, $n = 0$–2. There was reason to believe that complexes of this type could be formed with these ligands. Bimetallic complexes based on these ligands have been reported by several authors. Some examples are $[Rh_2(COD)_2(BiIm)]$,[8] $[Ir_4(CO)_8(BiIm)_2]$,[9] $[Cu_2(dien)_2(BiBzIm)](BPh_4)_2$,[10] $(NBu_4)_2[Pd_2(C_6F_5)_4(BiBzIm)]$,[11] $[(Mn(CO)_3PPh_3)_2(BiIm)]$,[12] $[(W(\eta\text{-}C_5H_5)_2)_2(BiIm)](PF_6)_2$,[13] and $[((bpy)_2Ru)_2BiBzIm](ClO_4)_2$.[14]

The biimidazole and bibenzimidazole ligands require deprotonation in order to form bidentate chelated complexes. In a related study Meyer and co-workers[15] studied the properties of

(1) Rillema, D. P.; Callahan, R. W.; Mack, K. B. *Inorg. Chem.* **1983**, *22*, 1617.
(2) Sahai, R.; Morgan, L.; Rillema, D. P. *Inorg. Chem.* **1988**, *27*, 3495.
(3) Sahai, R.; Rillema, D. P. *Inorg. Chim. Acta* **1986**, *118*, L32.
(4) Baucom, D. A.; Rillema, D. P. *Inorg. Chem.* **1986**, *25*, 3843.
(5) Sahai, R.; Rillema, D. P. *J. Chem. Soc., Chem. Commun.* **1986**, 1133.
(6) Sahai, R.; Rillema, D. P.; Shaver, R.; Van Wallendael, S.; Jackman, D. C.; Boldaji, M. *Inorg. Chem.* **1989**, *28*, 1022.
(7) Fuchs, Y.; Lofters, S.; Dieter, T.; Shi, W.; Morgan, R.; Strekas, T. C.; Gafney, H. D.; Baker, A. D. *J. Am. Chem. Soc.* **1987**, *109*, 2691.
(8) Kaiser, S. W.; Saillant, R. B.; Butler, W. M.; Rasmussen, P. G. *Inorg. Chem.* **1976**, *15*, 2681.
(9) Kaiser, S. W.; Saillant, R. B.; Butler, W. M.; Rasmussen, P. G. *Inorg. Chem.* **1976**, *15*, 2688.
(10) Huddad, M. S.; Hendrickson, D. H. *Inorg. Chem.* **1978**, *17*, 2622.
(11) Uson, R.; Gimeno, J.; Fornie, S.; Martinez, F. *Inorg. Chim. Acta* **1981**, *50*, 173.
(12) Uson, R.; Gimeno, J. *J. Organomet. Chem.* **1981**, *220*, 173.
(13) Calchorda, M. J.; Dias, A. R. *J. Organomet. Chem.* **1980**, *197*, 291.
(14) Haga, M.-A. *Inorg. Chim. Acta* **1980**, *45*, L183.
(15) Sullivan, B. P.; Salmon, D. J.; Meyer, T. J.; Peedin, J. *Inorg. Chem.* **1979**, *18*, 3369.

0020-1669/90/1329-0167$02.50/0

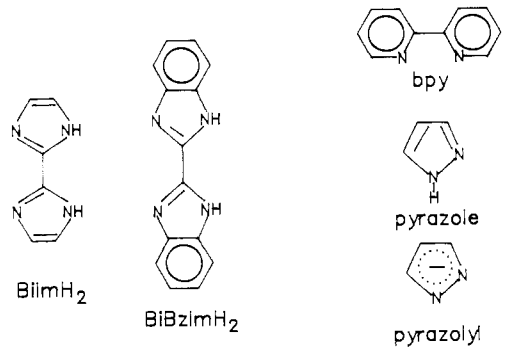

Figure 1. Ligands 2,2′-biimidazole ($BiImH_2$), 2,2′-bibenzimidazole ($BiBzImH_2$), and 2,2′-bipyridine (bpy).

ruthenium(II) bipyridine complexes containing pyrazole and pyrazolyl ligands (see Figure 1). The authors argued that the protonated form of the ligand (pyrazole) functioned as a π-donor; the deprotonated form (pyrazolyl) acted as a π-withdrawing ligand. In this study the spectroscopic and electrochemical properties of ruthenium(II) complexes containing biimidazole and bibenzimidazole in their protonated and deprotonated forms are investigated. Our focus is to ascertain the possibility of retaining similar luminescence properties in multimetallic complexes as found in their monometallic precursors. Such was recently found to be the case for ruthenium(II) complexes containing the 2,3-bis(2-pyridyl)pyrazine bridging ligand.[16]

Experimental Section

Materials. $RuCl_3 \cdot 3H_2O$ was a gift from Johnson-Matthey, Inc. $AgPF_6$ and $Ag(CF_3SO_3)$ were obtained from Aldrich Chemical Co. and/or Ventron Chemical Co. Tetraethylammonium perchlorate (TEAP) and tetrabutylammonium hexafluorophosphate (TBAH) were purchased from Southwestern Analytical, Inc., and used without further purification. TEAP was dried in the oven before it was used in the electrochemistry experiments. Acetonitrile (HPLC grade) was purchased from Aldrich or Fisher. Before use in electrochemistry experiments, the acetonitrile was dried over 4-Å molecular sieves whereas, for all other preparations and experiments, it was used as supplied. All other reagents were purchased commercially and used as received. Syntheses were carried out under a blanket of nitrogen; Schlenkware was used in the preparation of the triflate ($CF_3SO_3^-$) salts. Elemental analyses were obtained from Atlantic Microlab, Inc., Norcross, GA.

Preparations. The preparations of 2,2′-biimidazole ($BiImH_2$),[17] 2,2′-bibenzimidazole ($BiBzImH_2$),[18] $[Ru(bpy)_2Cl_2 \cdot 2H_2O$,[19] $Ru(bpy)Cl_4$,[20] $[Ru(BiBzImH_2)_3](PF_6)_2$,[21] $[Ru(BiBzImH_2)(bpy)_2](PF_6)_2$,[14] $[Ru(bpy)_2BiBzIm](PF_6)_2$,[14] and $[Ru(bpy)_2(BiImH_2)](PF_6)_2$[22] followed previously published procedures.

$[Ru(bpy)(BiImH_2)_2](PF_6)_2 \cdot 2H_2O$. $Ru(bpy)Cl_4$ (1.20 g, 3 mmol) was suspended in 50 mL of glycerol at 100 °C and the suspension stirred under nitrogen for 1.5 h. The black suspension turned dark red. Then 1.01 g (7.50 mmol) of biimidazole was added, and the solution was heated at 150 °C for 25 h. The deep dark red solution was cooled to room temperature, and 125 mL of ethanol was added to make the solution less viscous. Excess ligand was removed by vacuum filtration. Ethanol was then removed from the filtrate by rotary evaporation. The filtrate was then diluted with 200 mL of water, and an aqueous solution of saturated ammonium hexafluorophosphate was added dropwise until the complex ceased to precipitate from the solution. The complex was collected by vacuum filtration, dried under vacuum, and recrystallized from acetone. The yield was 85%.

$[Ru(bpy)(BiBzImH_2)_2](ClO_4)_2 \cdot 2H_2O$. $Ru(bpy)Cl_4$ (1.20 g, 3.00 mmol) was suspended in 50 mL of glycerol at 100 °C and the suspension stirred under nitrogen for 1.5 h. The black suspension turned dark red. Then 1.75 g (7.50 mmol) of $BiBzImH_2$ was added, and the solution was heated at 150 °C for 16 h. The deep dark red solution was cooled to room temperature, and 100 mL of ethanol was added to make the solution less viscous. Excess ligand was removed by vacuum filtration. A solution containing 3.00 g of $NaClO_4$ dissolved in 200 mL of water was added dropwise until precipitation was complete. The red precipitate was removed by vacuum filtration, washed with anhydrous ether, and dried under vacuum. It was then recrystallized from acetone. The yield was 63%. *Caution!* Perchlorate salts are potentially explosive.

$[Ru(BiImH_2)_3](PF_6)_2 \cdot 3H_2O$. Biimidazole (0.33 g, 2.50 mmol) and $RuCl_3 \cdot 3H_2O$ (0.13 g, 0.50 mmol) were mixed in 30 mL of a 2:1 ethanol/water mixture. The solution was heated under reflux and stirred under nitrogen for 12 h, during which time the solution became deep green. It was cooled to room temperature and filtrated. Saturated aqueous ammonium hexafluorophosphate was added dropwise to the filtrate, resulting in formation of a yellow-green precipitate. The precipitate was removed by vacuum filtration and redissolved in a minimum amount of acetonitrile, and the solution was chromatographed on a column of dimensions 5 cm in length × 0.75 cm in diameter containing silica gel as the stationary phase and acetonitrile as the eluent. The green material remained on the top of the column, and a yellow fraction eluted. The eluate was collected and concentrated on a rotary evaporator and was added dropwise to swirling anhydrous ether. The precipitate that formed was collected by vacuum filtration, washed with ether, and dried under vacuum. The yield was 59%.

$[(Ru(bpy)_2)_2BiIm](PF_6)_2 \cdot 2H_2O$. $[Ru(bpy)_2BiImH_2](PF_6)_2$ (0.34 g, 0.40 mmol) was dissolved in 50 mL of CH_3OH and then 2.0 mL of a 4.0 M $NaOCH_3$/methanol solution was added. The color of the solution turned from red to purple. After the solution was stirred under nitrogen for ~15 min, 0.26 g (0.50 mmol) $Ru(bpy)_2Cl_2 \cdot 2H_2O$ was added and the solution was refluxed under nitrogen for ~80 h. The resulting reddish brown solution was cooled. A reddish brown solid was removed by vacuum filtration, washed with ether, and dried under vacuum. Additional precipitate was obtained upon addition of saturated, aqueous ammonium hexafluorophosphate to the filtrate. It was collected by vacuum filtration and added to the first crop. The precipitate was dissolved in a minimum quantity of acetonitrile, and the solution was chromatographed over a neutral alumina column (~5 cm in length by 0.75 cm in diameter) previously developed with acetonitrile. A reddish brown band was collected and a blackish band that remained at the top of the column was discarded. The eluate was concentrated to ~10 mL on the rotary evaporator and then added to swirling anhydrous ether to precipitate the desired complex. It was then removed by vacuum filtration and dried under vacuum. The yield was 75%.

$[Ru(bpy)(BiBzImRu(bpy)_2)_2](ClO_4)_2 \cdot 2H_2O$. $[Ru(bpy)(BiBzImH_2)_2](ClO_4)_2$ (0.37 g, 0.40 mmol) was dissolved in 150 mL of CH_3OH, and then 4.0 mL of a 4.0 M $NaOCH_3$/methanol solution was added dropwise under a nitrogen blanket. The color of the solution turned from red to dark red. After the solution was stirred for 10 min, 0.45 g (0.86 mmol) of $Ru(bpy)_2Cl_2 \cdot 2H_2O$ was added and the resulting suspension was refluxed under nitrogen for 75 h. The solution was cooled to room temperature and filtered to remove insoluble impurities. A red precipitate was obtained upon dropwise addition of a saturated methanol solution of $NaClO_4$ to the filtrate. The precipitate was collected by filtration, washed with methanol and then ether, and dried under vacuum. The yield was 63%. *Caution!* Perchlorate salts are potentially explosive.

$[Ru(BiBzImRu(bpy)_2)_3](ClO_4)_3 \cdot 3H_2O$. $[Ru(BiBzImH_2)_3](ClO_4)_3 \cdot 2H_2O$ (0.41 g, 0.40 mmol) was dissolved in 150 mL of methanol. To this solution, 7.0 mL of a 4.0 M $NaOCH_3$/methanol solution was added dropwise under a N_2 blanket. The solution changed from red to purple. After the solution was stirred for 10 min, 0.70 g (1.34 mmol) of $Ru(bpy)_2Cl_2 \cdot 2H_2O$ was added to the solution and the resulting suspension was refluxed for 90 h. The solution was cooled to room temperature and filtered to remove insoluble impurities. A saturated methanol solution of $NaClO_4$ was added to the filtrate. The precipitate that formed was collected by vacuum filtration, washed with methanol and then ether, and dried under vacuum. The filtrate was further concentrated by rotary evaporation and then diluted with water to precipitate more of the desired product. It was collected as described previously and combined with the first fraction.

The isolated fractions were purified by column chromatography. The compound was dissolved in a minimum quantity of acetonitrile and the solution passed over a neutral alumina column as previously described above. The second fraction contained the desired product. It was collected, concentrated by rotary evaporation, and added to swirling ether to precipitate the desired complex. The yield was 74%. *Caution!* Perchlorate salts are potentially explosive.

$[Ru(bpy)_2BiBzImH_2](PF_6)_3$. This complex was prepared by the electrochemical oxidation of $[Ru(bpy)_2BiBzImH_2](PF_6)_2$ in a Vacuum Atmospheres glovebox. The bulk oxidation was carried out in a H-cell with

(16) Murphy, W. R., Jr.; Brewer, K. J.; Gettliffe, G.; Petersen, J. D. *Inorg. Chem.* **1989**, *28*, 81.
(17) Holmes, F.; Jones, K. M.; Torrible, E. G. *J. Chem. Soc.* **1961**, 4790.
(18) Fieselmann, B. F.; Hendrickson, D. N.; Stucky, G. D. *Inorg. Chem.* **1978**, *17*, 2078.
(19) Sprintschnik, G.; Sprintschnik, H. W.; Whitten, D. G. *J. Am. Chem. Soc.* **1976**, *98*, 2337.
(20) Krause, R. A. *Inorg. Chim. Acta* **1977**, *22*, 209.
(21) Haga, M.-A. *Inorg. Chim. Acta* **1983**, *77*, L39.
(22) Dose, E. V.; Wilson, L. J. *Inorg. Chem.* **1978**, *17*, 2660.

Scheme I. Comparative Preparative Chemistry

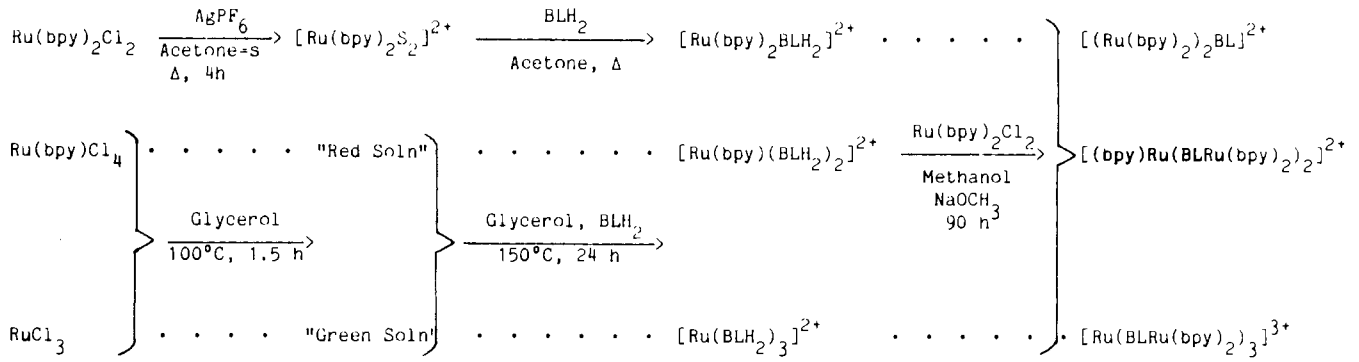

the compartments separated by two fine frits. Platinum gauze served as the working electrode, Pt mesh as the counter electrode, and silver/silver chloride as the reference electrode. A 1.0×10^{-2} M solution (10 mL) of $[Ru(bpy)_2BiBzImH_2](PF_6)_2$ in acetonitrile was placed in the central compartment and 0.20 M TBAH in acetonitrile was placed in both side compartments. The potential of the working electrode was set 100 mV positive to the $[Ru(bpy)_2BiBzImH_2]^{3+/2+}$ redox couple. Oxidation was allowed to proceed to a coulometric value of 1. During the electrolysis, the reddish brown solution turned dark bluish green. The dark bluish green solution was then added to anhydrous ether to precipitate the complex. The precipitate was collected by vacuum filtration by using Schenkware techniques and dried under vacuum. The yield was 73%.

Physical Measurements. Visible–UV–near-IR spectra were determined with a Perkin-Elmer Lambda Array 3840 UV/vis spectrophotometer or a Cary 14 instrument. Beer's law studies were carried out for absorption coefficient determinations at absorption maxima. At least five points were fitted to a linear least-squares program with resulting correlation coefficients of 0.999 and intercepts near zero.

Corrected emission spectra were determined with a SPEX F212 spectrofluorometer. Uncorrected emission spectra were determined with a Hitachi Perkin-Elmer 650-40 luminescence spectrophotometer. Emission quantum yields were determined in N_2-degassed acetonitrile solutions at 25 °C by the relative method using $[Ru(bpy)_3]^{2+}$ as the standard,[23] and calculations were carried out as previously described.[24] Luminescence lifetimes were determined in N_2-degassed acetonitrile solutions at room temperature by using a Molectron UV-400 nitrogen laser as the pulsed light source. The complete lifetime system was described earlier.[25]

Cyclic voltammetry measurements were performed in acetonitrile at a platinum-disk or glassy-carbon working electrode with 0.10 M TEAP or 0.10 M TBAH as the supporting electrolyte. The measurements were made vs the saturated sodium calomel electrode (SSCE). The measurements were made with a PAR 173 potentiostat in conjunction with a PAR 175 universal programmer or a PAR 174A polarographic analyzer modified with a supercycle for voltage control. The cyclic voltammograms were plotted on an IBM 742 X-Y-T recorder. Coulometry was effected with the PAR 173 potentiostat in conjunction with a PAR 176 digital coulometer. The SSCE and silver/silver chloride electrode served as reference electrodes. Electrolysis was performed in a Vacuum Atmospheres inert-atmosphere box, which contained a MO40-1 DriTrain and a RGF-1 regeneration flow system.

Differential-pulse polarograms were obtained with a PAR 174A polarographic analyzer. The polarograms were determined in 50/50 (v/v) aqueous buffer/acetonitrile solutions. The buffers were made from 0.200 M KCl, 0.100 M KHP (potassium hydrogen phthalate), 0.100 M KH_2PO_4, 0.025 M $Na_2B_4O_7 \cdot 10H_2O$, 0.050 M Na_2HPO_4, and 0.200 M NaOH in 0.500 M $NaNO_3$. The polarograms were determined at a glassy-carbon working electrode. A platinum wire served as the auxiliary electrode.

Solution conductivities were obtained in acetonitrile at 25 °C with a Beckman Model RC-18A conductivity bridge. The cell constant was determined by measuring the resistance of a 0.020 M KCl solution having a specific conductance of 0.002 768 Ω^{-1}.[26] The temperature of the solution was controlled with a Haake FK-2 constant-temperature bath.

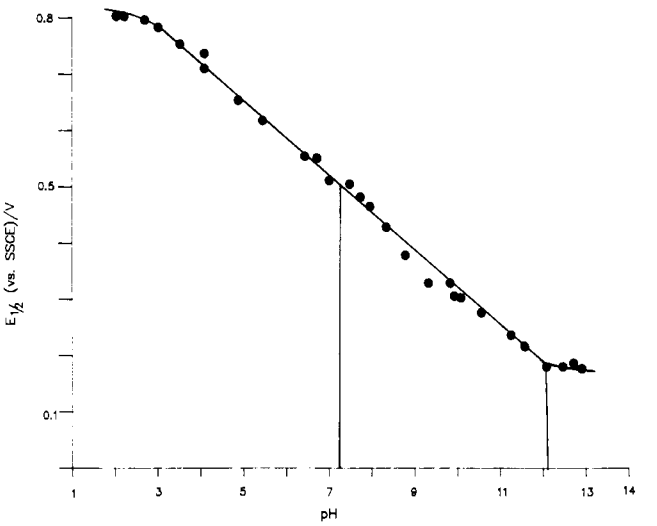

Figure 2. Potential of the $Ru^{3+/2+}$ redox couple for $[Ru(bpy)_2BiImH_2]^{2+}$ as a function of pH. The slope was 63 mV/decade, and the correlation coefficient was 0.999. The extrapolated values give $pK_1 = 7.2$ and $pK_2 = 12.1$.

Results

Preparations. Syntheses of the complexes are summarized in Scheme I. The sequence of steps used to prepare the bimetallic, trimetallic, and tetrametallic complexes are outlined for ready comparison. The procedure to prepare $[Ru(bpy)_2(acetone)_2]^{2+}$ from $Ru(bpy)_2Cl_2$ and its subsequent reaction to give the mixed-ligand complexes has been described previously.[27] Haga reported[21] that heating $RuCl_3$ in glycerol gave rise to a green intermediate, which then underwent further reaction with bibenzimidazole to give $[Ru(BiBzImH_2)_3]^{2+}$. Application of a similar procedure with $Ru(bpy)Cl_4$ resulted in a red intermediate species, which formed $[Ru(bpy)(BLH_2)_2]^{2+}$ upon reaction with excess BLH_2, where BLH_2 is $BiImH_2$ or $BiBzImH_2$. Deprotonation of $[Ru(bpy)_2(BLH_2)]^{2+}$, $[Ru(bpy)(BLH_2)_2]^{2+}$, and $[Ru(BLH_2)_3]^{2+}$ in methanol with sodium methoxide gave rise to purple solutions. The appropriate number of "$Ru(bpy)_2^{2+}$"[27] units were added to the solution containing the deprotonated species to produce the bimetallic, trimetallic, and tetrametallic complexes.

Sodium methoxide was used to deprotonate coordinated bibenzimidazole but was only effective for deprotonation of one biimidazole complex, $[Ru(bpy)_2(BiImH_2)]^{2+}$. The reason for this was attributed to the pK_a values for loss of consecutive protons from the ligands illustrated in eq 1 and 2. Previously, Haga

$$[Ru(bpy)_2(BiBzImH_2)]^{2+} \rightleftharpoons [Ru(bpy)_2(BiBzImH)]^{+} + H^{+} \quad (1)$$

$$[Ru(bpy)_2(BiBzImH)]^{+} \rightleftharpoons [Ru(bpy)_2(BiBzIm)] + H^{+} \quad (2)$$

reported[28] $pK_1 = 5.74$ and $pK_2 = 10.51$ for the consecutive

(23) Kober, E. M.; Meyer, T. J. *Inorg. Chem.* **1982**, *21*, 3967.
(24) Rillema, D. P.; Taghdiri, D. G.; Jones, D. S.; Keller, C. D.; Worl, L. A.; Meyer, T. J.; Levy, H. A. *Inorg. Chem.* **1987**, *26*, 578.
(25) Rillema, D. P.; Allen, G.; Meyer, T. J.; Conrad, D. *Inorg. Chem.* **1983**, *22*, 1617.
(26) Angelici, R. J. *Synthesis and Techniques in Inorganic Chemistry*, 2nd ed.; Saunders: Philadelphia, PA, 1977; p 17.
(27) Rillema, D. P.; Mack, K. B. *Inorg. Chem.* **1982**, *21*, 3849.
(28) Bond, A. M.; Haga, M.-A. *Inorg. Chem.* **1986**, *25*, 4507.

Table I. Cyclic Voltammetry Data for Ruthenium Biimidazole and Bibenzimidazole Complexes[a-c]

complex	oxidn			redn	
	$E_{1/2}(1)$	n_1[e]	$E_{1/2}(2)$	$E_{1/2}'(1)$	$E_{1/2}'(2)$
$[Ru(bpy)_2BiImH_2]^{2+}$[d]	1.04 (80)	1.09		−1.66 (80)	−1.96 (60)
$[Ru(bpy)(BiImH_2)_2]^{2+}$	0.80 (56)	1.04		−1.61[e,f]	
$[Ru(BiImH_2)_3]^{2+}$	0.54 (60)	0.98			
$[(Ru(bpy))_2BiIm]^{2+}$	0.75 (80)		1.09 (110)	−1.54 (120)	−1.84 (140)
$[Ru(bpy)_2(BiBzImH_2)]^{2+}$[d]	1.12 (70)	1.09		−1.60 (80)	−1.90 (80)
$[Ru(bpy)(BiBzImH_2)_2]^{2+}$	0.91 (70)	1.03		−1.48[f]	
$[Ru(BiBzImH_2)_3]^{2+}$[g]	0.80	1.04			
$[(Ru(bpy)_2)_2BiBzIm]^{2+}$	0.76 (60)[d]		1.04 (64)[d]	−1.49 (120)[e]	−1.78 (140)[e]
$[(bpy)Ru(BiBzImRu(bpy)_2)_2]^{2+}$	0.32 (70)		0.96 (150)	−1.53 (105)	−1.83 (150)
$[Ru(BiBzImRu(bpy)_2)_3]^{3+}$	−0.26 (80)	0.99	0.90 (180)	−1.56 (150)	−1.88 (137)
$[Ru(bpy)_2BiBzIm]$	0.36				
$[Ru(bpy)(BiBzIm)_2]^{2-}$	−0.21				
$[Ru(bpy)_3]^{2+}$	1.27			−1.31	−1.50

[a] Potentials are in volts vs SSCE, ±0.02 V. [b] Solutions were 0.1 M in TEAP or TBAH; solvent was acetonitrile. [c] The difference in anodic and cathodic peak potentials is given in parentheses. [d] Reference 30. [e] This work. [f] Quasireversible. [g] Reference 21.

equilibria illustrated by eq 1 and 2 in an acetonitrile/aqueous buffer matrix. As shown in Figure 2, the pK_a values for the analogous deprotonation reactions of $[Ru(bpy)_2BiImH_2]^{2+}$ are 7.2 and 12.1, respectively.

The technique used in this determination was differential-pulse polarography. In buffered media, equations relating $E_{1/2}$ to pH are available.[29] For the general reversible electrode reaction given by eq 3, where Ox is the oxidized species and Red is the reduced

$$Ox + ne^- + mH^+ \rightleftharpoons Red \quad (3)$$

species, the Nernst equation has the form presented in eq 4, where

$$E_{1/2} = E^\circ - \frac{0.059}{n} \log \left(\frac{D_{Ox}}{D_{Red}} \right)^{1/2} - 0.059\left(\frac{m}{n}\right)pH \quad (4)$$

$E_{1/2}$ is the polarographic half-wave potential, E° is the formal electrode potential, and D_{Ox} and D_{Red} are the respective diffusion coefficients of the oxidized and reduced species. If the assumption $D_{Ox} = D_{Red}$ is applied, eq 4 reduces to eq 5. Over the pH range

$$E_{1/2} = E^\circ - 0.059\left(\frac{m}{n}\right)pH \quad (5)$$

from 2.5 to 12 in Figure 2, the slope of $E_{1/2}$ vs pH was 63 mV/pH unit (correlation coefficient 0.999). The slope is consistent with a one-electron/one-proton process with no observed break between loss of the first and second protons. The pK_a values are shown by extrapolation in the figure and are consistent with those reported by Haga.[30] The second deprotonation of $[Ru(bpy)_2(BiImH_2)]^{2+}$ was difficult, as evidenced by the large pK_2 value. Consequently, efforts to form the trimetallic and tetrametallic oligomers based on biimidazole as the bridging ligand were unsuccessful.

Conductivity. Dilution conductivity studies were carried out by procedures previously described.[31] For strong electrolytes, the equivalent conductance, Λ_e, is expected to vary linearly with the square root of the equivalent concentration.[32] According to eq 6, a plot of $\Lambda_0 - \Lambda_e$, where Λ_0 is the equivalent conductance

$$\Lambda_0 - \Lambda_e = AC_{eq}^{1/2} \quad (6)$$

at infinite dilution, vs $C_{eq}^{1/2}$ will result in a straight line indicative of the electrolyte type.[2,32-34] The bimetallic and trimetallic complexes are 2:1 electrolytes (+2 charged cation, −1 charged anion); the tetrametallic complex is a 3:1 electrolyte (+3 charged cation, −1 charged anion). Experimental slopes have generally been less than theoretical values for other similar systems.[2] Such is the case here as well. The experimental slopes for the bimetallic and trimetallic complexes were in the 575–650 (±35) mhos $L^{1/2}$ $equiv^{-1/2}$ range; the tetrametallic complex was 792 ± 65 mhos $L^{1/2}$ $equiv^{-1/2}$. The theoretical values determined by the Onsager equation were 700 ± 23 mhos $L^{1/2}$ $equiv^{-1/2}$ for the 2:1 electrolytes and 964 mhos $L^{1/2}$ $equiv^{-1/2}$ for the 3:1 electrolyte.

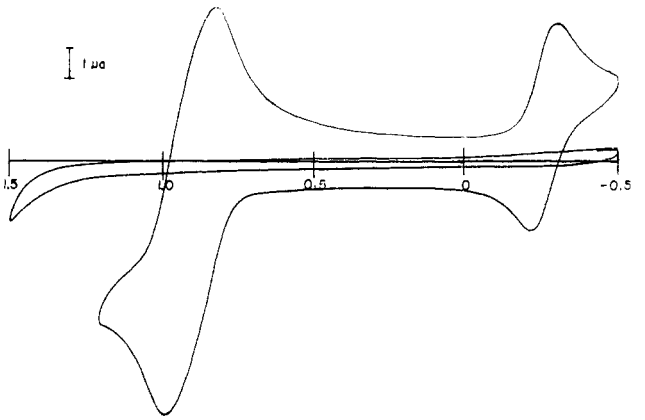

Figure 3. Cyclic voltammogram of $[Ru(BiBzImRu(bpy)_2)_3]^{3+}$ in acetonitrile over the potential range 1.3 to −0.5 V vs SSCE. The scanning rate was 200 mV/s.

Electrochemistry. Redox potentials were determined by cyclic voltammetry and are tabulated in Table I. Cyclic voltammograms of all the complexes were obtained in dry acetonitrile by using TEAP and TBAH as the electrolytes and were recorded at sweep rates ranging from 20 to 1000 mV/s. The ΔE_p values obtained from extrapolation of ΔE_p vs the square root of the scan rate are given in parenthesis next to the corresponding $E_{1/2}$ values in Table I.[35] Oxidation of ruthenium(II) centers was observed in the positive region, whereas reduction of coordinated ligands occurred in the negative region, with one exception. A ruthenium-based oxidation for $[Ru(BiBzImRu(bpy)_2)_3]^{2+}$ was observed at a negative potential. In addition, n values were obtained for a number of the oxidations labeled $E_{1/2}(1)$ and are also listed in Table I.

$E_{1/2}(1)$ entries in Table I correspond to the half-reaction Ru(III) + $e^- \rightarrow$ Ru(II). The n values support the assignment of a one-electron-transfer process. The reversibility of the processes were indicated by i_a/i_c ratios near 1 and peak spacings of approximately 60 mV.[36] The $E_{1/2}(1)$ values for monometallic complexes follow the sequence $[Ru(BLH_2)(bpy)_2]^{2+} > [Ru(BLH_2)_2(bpy)]^{2+} > [Ru(BLH_2)_3]^{2+}$, where BLH_2 is either $BiBzImH_2$ or $BiImH_2$. Further, it is noted that $E_{1/2}(1)$ values for analogous $BiBzImH_2$-based complexes are more positive than $BiImH_2$-based

(29) Kolthoff, I. M.; Lingane, J. *Polarography*; Interscience: New York, 1952; p 246.
(30) Haga, M.-A. *Inorg. Chim. Acta* **1983**, *75*, 29.
(31) Rillema, D. P.; Callahan, R. W.; Mack, K. B. *Inorg. Chem.* **1982**, *21*, 2589.
(32) Boggess, R. K.; Zatko, D. A. *J. Chem. Educ.* **1975**, *52*, 649.
(33) Feltham, R. D.; Heyter, R. G. *J. Chem. Soc.* **1964**, 4587.
(34) Weaver, T. R.; Meyer, T. J.; Adeyemi, S. A.; Brown, G. M.; Eckberg, R. P.; Hatfield, W. E.; Johnson, E. C.; Murray, R. W.; Unterecker, D. *J. Am. Chem. Soc.* **1975**, *97*, 3039.

(35) $\Delta E_p = |E_{p,ox} - E_{p,red}|$.
(36) Nicholson, R. S.; Shain, I. *Anal. Chem.* **1964**, *36*, 705.

complexes, e.g. $E_{1/2}([Ru(BiBzImH_2)_3]^{3+/2+}) > E_{1/2}([Ru(BiImH_2)_3]^{3+/2+})$. These results indicate $BiImH_2$ is a stronger σ-donor than $BiBzImH_2$. The systematic negative shift as bpy is replaced by BLH_2 results from an increase in electron density on the ruthenium metal center.[37]

Two redox processes assignable to the metal centers are observed for multimetallic complexes as shown in Figure 3. For bimetallic complexes, $E_{1/2}(1)$ corresponds to removal of one electron from one metal center followed by removal of one electron from a second metal center labeled $E_{1/2}(2)$. For the trimetallic and tetrametallic complexes, the current and ΔE_p values for the more positive redox process ($E_{1/2}(2)$) increase relative to $E_{1/2}(1)$. The current ratio of $E_{1/2}(2)$ to $E_{1/2}(1)$ for the trimetallic complex is 2:1; for the tetrametallic complex the ratio is 3:1. Thus, $E_{1/2}(2)$ most likely corresponds to two closely spaced one-electron processes for the trimetallic complex and the three closely spaced one-electron processes for the tetrametallic process. $E_{1/2}(1)$ then corresponds to a redox couple associated with the central ruthenium and $E_{1/2}(2)$ to redox couplex associated with outer ruthenium centers, as illustrated by eq 7–10.

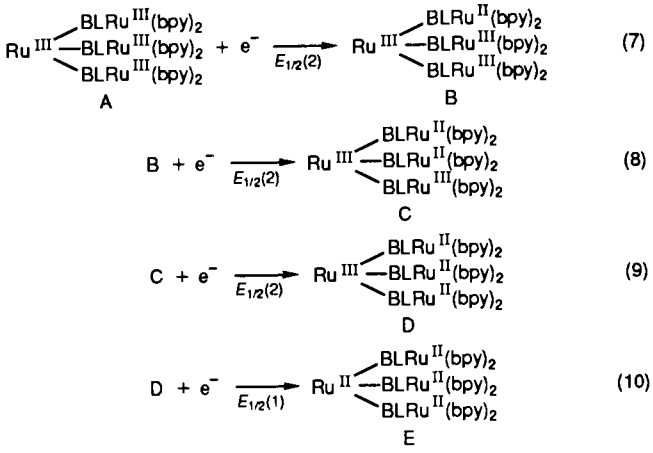

$$Ru^{III}(BLRu^{III}(bpy)_2)_3 + e^- \xrightarrow{E_{1/2}(2)} Ru^{III}(BLRu^{III}(bpy)_2)_2(BLRu^{II}(bpy)_2) \quad (7)$$

A B

$$B + e^- \xrightarrow{E_{1/2}(2)} Ru^{III}(BLRu^{III}(bpy)_2)(BLRu^{II}(bpy)_2)_2 \quad (8)$$

C

$$C + e^- \xrightarrow{E_{1/2}(2)} Ru^{III}(BLRu^{II}(bpy)_2)_3 \quad (9)$$

D

$$D + e^- \xrightarrow{E_{1/2}(1)} Ru^{II}(BLRu^{II}(bpy)_2)_3 \quad (10)$$

E

According to the data in Table I, $E_{1/2}(1)$ values for the multimetallic complexes are more negative than their monometallic precursors. Both $E_{1/2}(1)$ and $E_{1/2}(2)$ for $BiBzImH_2$-based complexes follow the order $[(Ru(bpy)_2)_2BiBzIm]^{2+} > [(bpy)Ru(BiBzImRu(bpy)_2)_2]^{2+} > [Ru(BiBzImRu(bpy)_2)_3]^{2+}$. This ordering is opposed to that found for analogous complexes bridged by 2,2′-bipyrimidine (bpm) and 2,3-bis(2-pyridyl)quinoxaline (bpq), e.g. $Ru(bpm)_3^{3+/2+}$ ($E_{1/2}$ = 1.69 V) < $Ru(bpy)(bpm)_2^{3+/2}$ ($E_{1/2}$ = 1.55 V) < $(Ru(bpy)_3(bpm)^{3+/2+}$ ($E_{1/2}$ = 1.80 V).[2] In contrast to bpm and bpq, BLH_2 ligands require deprotonation to function as bridging ligands. The deprotonated species BL^{2-} acts as a stronger electron donor than the protonated BLH_2 ligand and shifts more electron density onto the ruthenium center. This is noted by the increase spacing between $E_{1/2}(2)$ and $E_{1/2}(1)$ as follows: 0.28 V for $[(Ru(bpy)_2)_2BiBzIm]^{2+}$, 0.64 V for $[(bpy)Ru(BiBzImRu(bpy)_2)_2]^{2+}$, and 1.16 V for $[Ru(BiBzImRu(bpy)_2)_3]^{2+}$.

The redox activity in the negative potential region varied. No redox reactivity was found for tris chelates in the range 0 to −2 V vs SSCE whereas mixed-ligand complexes were redox active. By analogy to $[Ru(bpy)_3]^{2+}$, the reductions associated with the mixed-ligand complexes can be assigned to reduction of the coordinated bipyridine ligands.[25] The two successive reductions of $[Ru(bpy)_2BiBzImH_2]^{2+}$ are illustrated in eq 11 and 12. For the

$$[Ru(bpy)(bpy)(BiImH_2)]^{2+} + e^- \xrightarrow{E_{1/2}'(1)} [Ru(bpy)(bpy^-)(BiBzImH_2)]^+ \quad (11)$$

$$[Ru(bpy)(bpy^-)(BiImH_2)]^+ + e^- \xrightarrow{E_{1/2}'(2)} [Ru(bpy^-)(bpy^-)(BiBzImH_2)] \quad (12)$$

(37) Rillema, D. P.; Endicott, J. F.; Papaconstantinou, E. *Inorg. Chem.* **1971**, *10*, 1739.

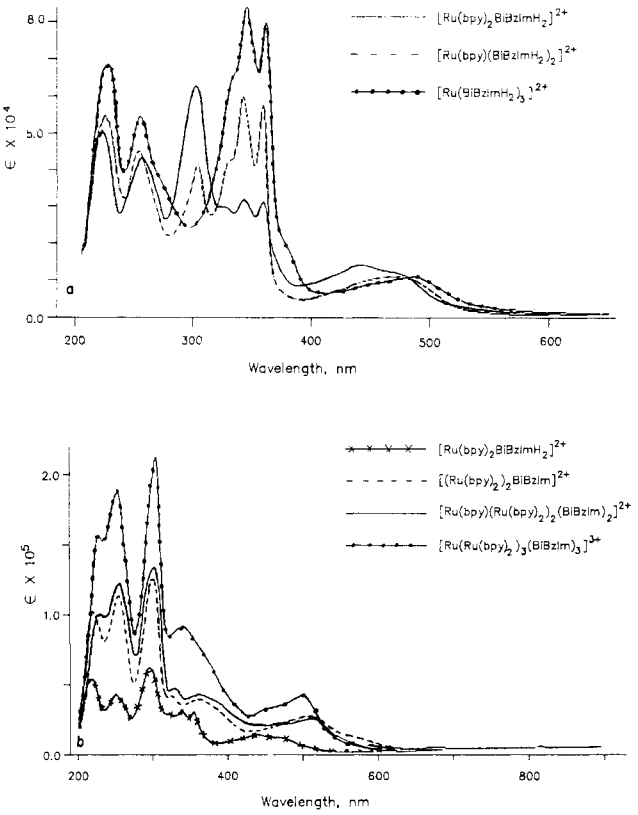

Figure 4. Visible–UV spectral comparison of $BiBzImH_2$-based complexes: (a) $[Ru(bpy)_n(BiBzImH_2)_{3-n}]^{2+}$, n = 0–2, series; (b) $[Ru(bpy)_n(BiBzImRu(bpy)_2)_{3-n}]^{2+}$, n = 0–2, series.

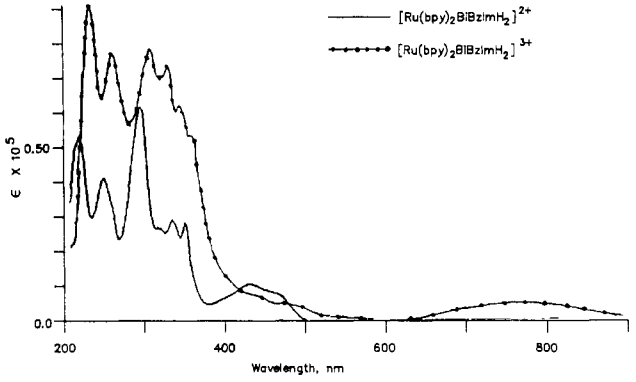

Figure 5. Visible–UV spectral comparison of $[Ru(bpy)_2BiBzImH_2]^{2+}$ and $[Ru(bpy)_2BiBzImH_2]^{3+}$ in acetonitrile.

trimetallic and tetrametallic complexes, two reductions were also observed. The ΔE_p spacings and increased currents suggest that more than one single electron-transfer step occurs at each wave. Relative to $E_{1/2}(1)$, the currents for $E_{1/2}'(1)$ and $E_{1/2}'(2)$ were 2 times greater for the trimetallic complex and 3 times greater for the tetrametallic complex. This is certainly plausible given the presence of more than one "$Ru(bpy)_2^{2+n}$" unit. Coulometry was attempted to determine the n value for $E_{1/2}'(1)$, but $E_{1/2}'(1)$ and $E_{1/2}'(2)$ were too close to affect the experiment. However, qualitatively one would note that $E_{1/2}'(1)$ and $E_{1/2}'(2)$ are more negative than potentials for similar processes associated with $[Ru(bpy)_3]^{2+}$ and follow the sequence $[(Ru(bpy)_2)_2BiBzIm]^{2+} > [(bpy)Ru(BiBzImRu(bpy)_2)_2]^{2+} > [Ru(BiBzImRu(bpy)_2)_3]^{2+}$ for the multimetallic complexes.

Visible–UV Spectra. Visible–UV spectral comparisons are illustrated in Figures 4–6, and the accumulated data are summarized in Table II. The optical transitions have been separated into those related to $d\pi \rightarrow \pi^*$ transitions and those characteristic to $\pi \rightarrow \pi^*$ transitions. For mixed-ligand complexes, it is difficult to make assignments related to the specific ligand involved in the transition. The optical transitions are often overlapping bands

Table II. Visible–UV Spectral Data for Ruthenium(II) Bibenzimidazole and Biimidazole Complexes[a]

complex	$d\pi \rightarrow \pi_1^*$	$d\pi \rightarrow \pi_2^*$	$\pi \rightarrow \pi^*$ (BiBzIm)	$\pi \rightarrow \pi^*$
$[Ru(bpy)_2BiBzImH_2]^{2+}$ [b]	463 (1.2 × 10^4), 438 (1.3 × 10^4)		350 (4.4 × 10^4), 332 (3.7 × 10^4)	291 (6.2 × 10^4), 243 (3.8 × 10^4)
$[Ru(bpy)(BiBzImH_2)_2]^{2+}$	465 (1.1 × 10^4)		350 (4.9 × 10^4), 332 (5.4 × 10^4)	292 (3.8 × 10^4), 245 (4.2 × 10^4)
$[Ru(BiBzImH_2)_3]^{2+}$ [c]	483 (1.0 × 10^4)		351 (2.3 × 10^4), 333 (7.4 × 10^4)	242 (5.0 × 10^4)
$[(Ru(bpy)_2)_2BiBzIm]^{2+}$	512 (2.0 × 10^4)	357 (3.0 × 10^4)		296 (1.3 × 10^5), 244 (1.1 × 10^5)
$[(bpy)Ru(BiBzImRu(bpy)_2)_2]^{2+}$	513 (2.3 × 10^4)	375 (3.3 × 10^4), 357 (3.5 × 10^4), 326 (4.3 × 10^4)		296 (1.4 × 10^5), 246 (1.4 × 10^5)
$[Ru(BiBzImRu(bpy)_2)_3]^{3+}$	498 (4.3 × 10^4), 462 (1.4 × 10^4)	333 (8.9 × 10^4)		296 (2.2 × 10^5), 245 (1.9 × 10^5)
$BiBzImH_2$				309 (1.1 × 10^5)
$[Ru(bpy)_2BiImH_2]^{2+}$ [b]	473 (9.3 × 10^3), 432 (7.1 × 10^3)	340 (1.1 × 10^4)		289 (6.0 × 10^4), 242 (2.3 × 10^4)
$[Ru(bpy)(BiImH_2)_2]^{2+}$	487 (5.0 × 10^3)	366 (8.8 × 10^3)		294 (3.3 × 10^4), 287 (3.3 × 10^4), 248 (1.9 × 10^4)
$[Ru(BiImH_2)_3]^{2+}$	401 (1.2 × 10^4)			297 (2.8 × 10^4), 285 (3.5 × 10^4), 276 (3.3 × 10^4)
$[(Ru(bpy)_2)_2BiIm]^{2+}$	498 (2.1 × 10^4)	336 (2.2 × 10^4)		293 (8.6 × 10^4), 246 (4.7 × 10^4)
$BiImH_2$				276 (1.8 × 10^4)

[a] λ_{max} in nm, ±1 nm; ϵ in parentheses, M^{-1} cm^{-1}; T = 20 ± 1 °C; solvent was 1 × 10^{-3} M HCF_3SO_3 in acetonitrile. [b] Reference 30. [c] Reference 21.

and difficult to deconvolute into their components. Even the simplest case is complex. For example, $[Ru(bpy)_3]^{2+}$ gives rise to a low-energy transition labeled $d\pi \rightarrow \pi_1^*$ and a second transition at 6000 cm^{-1} higher energy labeled $d\pi \rightarrow \pi_2^*$.[38]

The spectral changes associated with the $[Ru(bpy)_n(BiBzImH_2)_{3-n}]^{2+}$, n = 0–2, series are illustrated in Figure 4a. The low-energy bands are related to $d\pi \rightarrow \pi^*$ transitions and are found to red shift as bpy is replaced by $BiBzImH_2$. For $[Ru(BiBzImH_2)_3]^{2+}$, the absorption located at 483 nm can be assigned as a $d\pi \rightarrow \pi^*(BiBzImH_2)$ transition. However, for $[Ru(bpy)(BiBzImH_2)_2]^{2+}$ and $[Ru(bpy)_2(BiBzImH_2)]^{2+}$, the low-energy maxima are more likely related to $d\pi \rightarrow \pi^*(bpy)$ due to the fact that coordinated bpy is reduced electrochemically rather than coordinated $BiBzImH_2$. The red shift of the low-energy MLCT absorption maxima between $[Ru(bpy)(BiBzImH_2)_2]^{2+}$ and $[Ru(bpy)_2(BiBzImH_2)]^{2+}$ is only 2 nm whereas the red shift between the maxima of these two compounds and $[Ru(BiBzImH_2)_3]^{2+}$ is ~20 nm. This rather large shift could be explained by loss of the $d\pi \rightarrow \pi^*(bpy)$ component or by an increaser in steric crowding around each ruthenium center. The $\pi \rightarrow \pi^*$ transitions related to the bpy and $BiBzImH_2$ ligands are also apparent from the near-UV spectral comparison. Two bands located at 332 and 300 nm systematically increase in intensity as $BiBzImH_2$ is replaced by bpy. At the same time, the band at 291 nm decreases in intensity. Thus, the transitions located at 332 and 350 nm are assigned as $\pi \rightarrow \pi^*(BiBzImH_2)$ and the 291-nm band is assigned as $\pi \rightarrow \pi^*(bpy)$. The far-UV bands appear to be related to transitions involving both ligands.

Spectral changes related to $BiBzIm^{2-}$-based multimetallic complexes are illustrated in Figure 4b. The following features are noted: (1) The $\pi \rightarrow \pi^*(BiBzImH_2)$ transitions found in the $[Ru(bpy)_n(BiBzImH_2)_{3-n}]^{2+}$, n = 0–2, complexes are lost. (2) The intensity of the low-energy transition appears to be related to the number of $Ru(bpy)_2^{2+}$ units, suggesting that this transition arises from these components and, on the basis of the discussion above, can be assigned as $d\pi \rightarrow \pi^*(bpy)$. (3) The spectral activity in the 350-nm region consists of overlapping metal to ligand charge-transfer (MLCT) bands. There also appears to be an enhancement of the transition at 333 nm for the tetrametallic complex, which may be due in part to the ruthenium(III) core. (4) The absorption maximum at 296 nm has as its primary origin $\pi \rightarrow \pi^*(bpy)$ transitions, as outlined above. The relative intensities are in accord with this assignment on the basis of the number of bipyridine ligands in each compound. As noted from the stoichiometry of the complexes, the monometallic complex has two bipyridine ligands, the bimetallic complex has four, the trimetallic complex has five, and the tetrametallic complex has six. (5) The

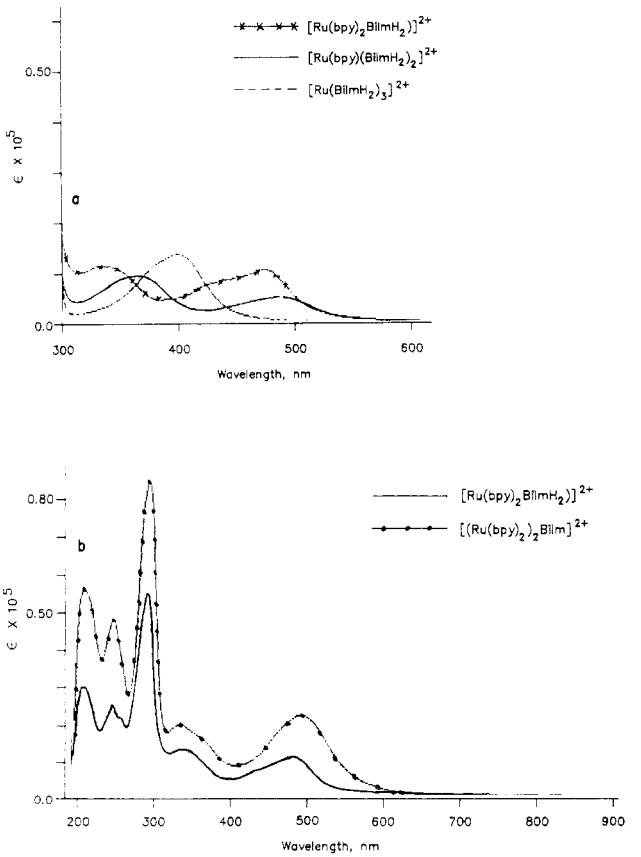

Figure 6. Visible–UV spectral comparison of $BiImH_2$-based complexes: (a) $[Ru(bpy)_n(BiImH_2)_{3-n}]^{2+}$, n = 0–2, series; (b) $[Ru(bpy)_2BiImH_2]^{2+}$ and $[(Ru(bpy)_2)_2BiIm]^{2+}$.

(38) (a) Felix, F.; Ferguson, J.; Gudel, H. U.; Ludi, A. *J. Am. Chem. Soc.* **1980**, *102*, 4086. (b) Descurtius, S.; Felix, F.; Ferguson, J.; Gudel, H.; Ludi, A. *Ibid.* **1980**, *102*, 4102. (c) Kober, E. M.; Meyer, T. J. *Inorg. Chem.* **1982**, *21*, 3967.

final UV transitions increase in a systematic manner as the number of heterocyclic ligands increase and most likely are overlapping $\pi \rightarrow \pi^*$ transitions associated with both bpy and $BiBzImH_2$ ligands.

Figure 5 illustrates the spectral changes that occur upon oxidation of $[Ru(bpy)_2BiBzImH_2]^{2+}$ to $[Ru(bpy)_2BiBzImH_2]^{3+}$. The primary differences are loss of the MLCT band centered at 463 nm and the appearance of a new band in the near-infrared region at 780 nm. This new band is broad and less intense than the 463-nm band. It is most likely a ligand to metal charge transfer ($\pi \rightarrow d\pi$). Since the $\pi \rightarrow \pi^*$ transition of the $BiBzImH_2$ ligand occurs at lower energy than the $\pi \rightarrow \pi$ transition of the bipyridine ligand and the fact that the bipyridine ligand is reduced prior to reduction of $BiBzImH_2$, it follows that the near-infrared transition is most likely a $\pi(BiBzImH_2) \rightarrow d\pi$ process.

The behavior of $BiImH_2$-based complexes is somewhat different from the changes found for analogous monometallic $BiBzImH_2$ complexes. The low-energy transition of $[Ru(BiImH_2)_3]^{2+}$ is observed at 401 nm compared to 483 nm for $[Ru(BiBzImH_2)_3]^{2+}$. The energy maximum is also at higher energy than for $[Ru(bpy)_3]^{2+}$, which is found at 451 nm.[39] As shown in Figure 6a, the optical transitions in the 350–500-nm region have behavior reminiscent of MLCT processes found for similar heterocyclic ligand complexes.[2,25] However, the energy ordering of the low-energy bands are different from the systematic differences typically found in $[Ru(bpy)_x(L\text{-}L)_{3-x}]^{2+}$ complexes, where L-L represents a bidentate heterocyclic ligand and $x = 0$–3. Instead of a smooth shift as bpy is replaced by L-L, the low-energy MLCT maxima follow the order $[Ru(BiImH_2)_3]^{2+} > [Ru(bpy)_2BiImH_2]^{2+} > [Ru(bpy)(BiImH_2)_2]^{2+}$. For $[Ru(bpy)_2(BiImH_2)]^{2+}$, the molar absorption coefficient of the low-energy transition is approximately twice that of $[Ru(bpy)(BiBzImH_2)_2]^{2+}$. This indicates that the transition is related to the $d\pi \rightarrow \pi^*_1(bpy)$ process and, further, that the $d\pi \rightarrow \pi^*(BiImH_2)$ transitions in these complexes are blue-shifted. For the higher energy MLCT bands, the problem is more complex due to the fact that more than one $d\pi \rightarrow \pi^*$ transition is expected, a $d\pi \rightarrow \pi_1^*$ and a $d\pi \rightarrow \pi^*_2$ transition, as discussed previously. Thus, the band centered at 366 nm for $[Ru(bpy)(BiImH_2)_2]^{2+}$ and the one centered at 340 nm for $[Ru(bpy)_2(BiImH_2)]^{2+}$ are most likely overlapping bands consisting of $d\pi \rightarrow \pi^*(BiImH_2)$ and $d\pi \rightarrow \pi^*_2(bpy)$ transitions. Nevertheless, the higher energy MLCT band maximum shifts progressively from 340 to 360 to 401 nm as n increases, which may be related to the increasing importance of the $d\pi \rightarrow \pi^*(BiImH_2)$ transition.

The visible–UV spectra for $[Ru(bpy)_2BiImH_2]^{2+}$ and $[(Ru(bpy)_2)_2BiIm]^{2+}$ are compared in Figure 6b. As expected, the absorption coefficients are approximately double for the bimetallic complex. The low-energy transition shifts from 473 to 498 nm upon dimer formation. This shift is small compared to most bimetallic complexes containing neutral heterocyclic bridging ligands, where red shifts on the order of 100 nm often are found upon formation of bimetallic complexes.[25]

Near-Infrared Spectra. Each of the Ru(II) monometallic complexes was electrochemically oxidized to the Ru(III) form, and the near-infrared spectrum was obtained in acetonitrile solutions containing 0.1 M electrolyte. The position maxima and the corresponding molar absorption coefficients were as follows: $[Ru(BiImH_2)_3]^{3+}$, $\lambda_{max} = 760$ nm ($\epsilon = 2.5 \times 10^3$ M^{-1} cm^{-1}); $[Ru(bpy)(BiImH_2)_2]^{3+}$, $\lambda_{max} = 853$ nm ($\epsilon = 2.1 \times 10^3$ M^{-1} cm^{-1}); $[Ru(bpy)_2(BiImH_2)]^{3+}$, $\lambda_{max} = 1000$ nm ($\epsilon = 0.8 \times 10^3$ M^{-1} cm^{-1}); $[Ru(BiBzImH_2)_3]^{3+}$, $\lambda_{max} = 745$ nm ($\epsilon = 2.0 \times 10^3$ M^{-1} cm^{-1}); $[Ru(bpy)(BiBzImH_2)_2]^{3+}$, $\lambda_{max} = 820$ nm ($\epsilon = 1.9 \times 10^3$ M^{-1} cm^{-1}); $[Ru(bpy)_2BiBzImH_2]^{3+}$, $\lambda_{max} = 780$ nm ($\epsilon = 9.9 \times 10^2$ M^{-1} cm^{-1}). The energy maxima for $BiImH_2$-based complexes follow the sequence $[Ru(BiImH_2)_3]^{3+} > [Ru(bpy)(BiImH_2)_2]^{3+} > [Ru(bpy)_2(BiImH_2)]^{3+}$; those for $BiBzImH_2$-based systems follow the order $[Ru(BiBzImH_2)_3]^{3+} > [Ru(bpy)_2(BiBzImH_2)]^{3+} > [Ru(bpy)(BiBzImH_2)_2]^{3+}$. The absorption envelopes were broad. Half-width at full maximum for the band located at 780 nm was on the order of 4×10^3 cm^{-1} for $[Ru(bpy)_2BiBzImH_2]^{3+}$ in solution without electrolyte.

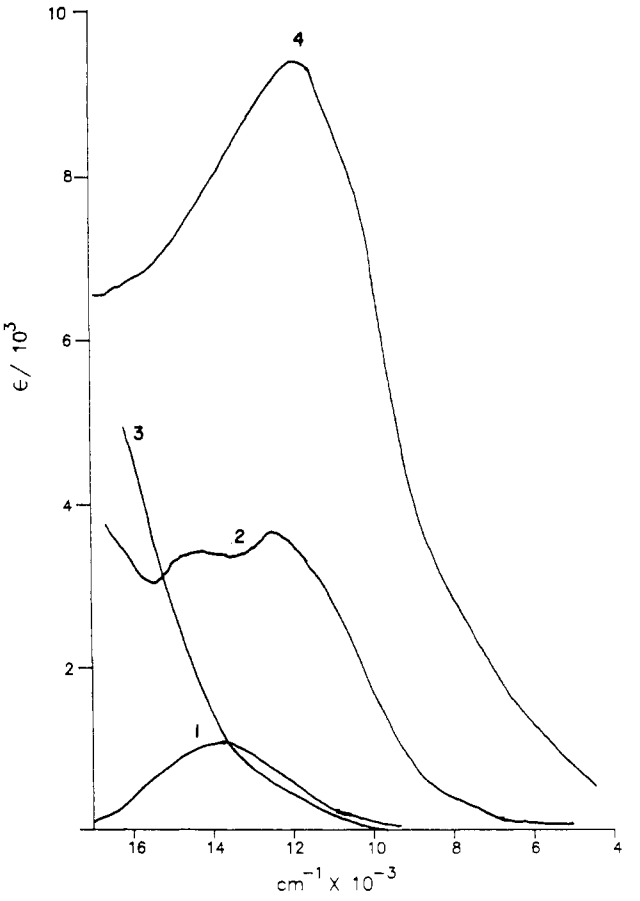

Figure 7. Near-infrared spectral comparison of (1) $[Ru^{III}(bpy)_2BiBzImH_2]^{3+}$, (2) $[Ru^{III}(BiBzImRu^{II}(bpy)_2)_3]^{3+}$, (3) $[Ru^{II}(BiBzImRu^{II}(bpy)_2)_3]^{2+}$, and (4) $[Ru^{III}(BiBzImRu^{III}(bpy)_2)_3]^{6+}$.

The near-infrared spectrum of $[Ru^{III}(BiBzImRu^{II}(bpy)_2)_3]^{3+}$ is shown in Figure 7; its absorption maximum is located at 820 nm (12.2×10^3 cm^{-1}). Reduction of the central ruthenium from the +3 to the +2 oxidation state resulted in loss of this absorbance, as illustrated in Figure 7. However, oxidation of the oligomer by three electrons resulted in an absorbance increase with a shift in the absorption maximum to 11.8×10^3 cm^{-1}. The oligomer was difficult to rapidly oxidize due to a competitive side reaction with solvent. Consequently, the absorption coefficient for $[Ru^{III}(BiBzImRu^{III}(bpy)_2)_3]^{6+}$ at 11.8×10^3 cm^{-1} represents a lower limit.

For $[Ru(bpy)_2(BiBzImH_2)]^{3+}$, the origin of the near-infrared transition was previously described as LMCT. In addition to this possibility, mixed-valent complexes such as $[Ru^{III}(BiBzImRu^{II}(bpy)_2)_3]^{3+}$ could also undergo intervalence electron transfer, which is often observed in the near-infrared spectrum. A test for this is the solvent dependence of the near-infrared absorption band. Plots of E_{op} vs $1/\eta^2 - 1/\epsilon$, where η is the index of refraction and ϵ is the dielectric constant of the solvent, are expected to be linear.[40] As a control, the solvent dependence of the near-infrared absorption band of $[Ru(bpy)_2(BiBzImH_2)]^{3+}$ was examined. It showed little solvent dependence. However, the band at 12.2×10^{-3} cm^{-1} for $[Ru^{III}(BiBzImRu^{II}(bpy)_2)_3]^{3+}$ shifted in various solvents, as shown in Figure 8. The slope of the plot was 4.91, and the correlation coefficient was 0.994. The overall E_{op} shifts are only 0.5×10^3 cm^{-1} compared to 1–2×10^3 cm^{-1} reported by Meyer and co-workers[41] for $[(bpy)_2ClRu^{II}(pyr)Ru^{III}(NH_3)_5]^{4+}$, where pyr is pyrazine, in similar solvents. Due to the unusual nature of the absorption manifold, it is difficult to determine

(39) Crutchley, R. J.; Lever, A. B. P. *Inorg. Chem.* **1982**, *21*, 2276.

(40) Hush, N. S. *Prog. Inorg. Chem.* **1967**, *8*, 391.

(41) Powers, M.; Callahan, R. W.; Salmon, D. J.; Meyer, T. J. *Inorg. Chem.* **1976**, *15*, 1457.

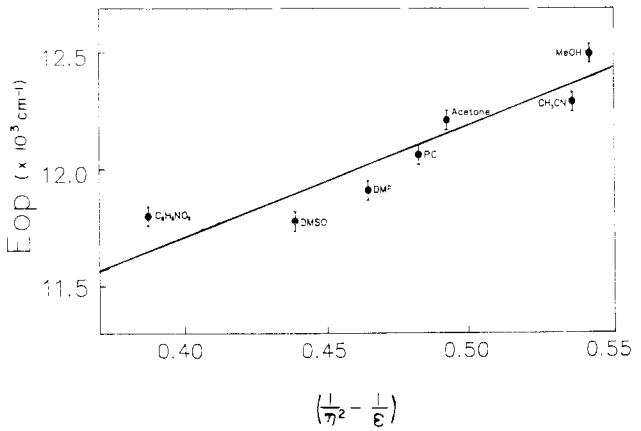

Figure 8. Solvent dependence of the near-infrared absorption band for $[Ru^{III}(BiBzImRu^{II}(bpy)_2)_3]^{3+}$ located at 12.2×10^3 cm^{-1}. PC is the abbreviation for propylene carbonate. E_{op} is the energy maximum, η the index of refraction for the solvent, and ϵ the static dielectric constant of the solvent.

Table III. Luminescence Properties of Biimidazole and Bibenzimidazole Complexes[a,b]

complex	λ_{em}, nm[c] (298 °C)	λ_{em}, nm[d] (77 K)	τ_0, ns[e] (298 °C)	ϕ_r[f]
$[Ru(bpy)_2BiImH_2]^{2+}$	683	620, 670 (sh)	161	2.5×10^{-3}
$[Ru(bpy)(BiImH_2)_2]^{2+}$	724	620, 675	64	4.1×10^{-4}
$[(Ru(bpy)_2)_2BiIm]^{2+}$	738	680	37	4.7×10^{-4}
$[Ru(bpy)_2BiBzImH_2]^{2+}$	666	616, 659	131	1.9×10^{-3}
$[Ru(bpy)(BiBzImH_2)_2]^{2+}$	711	647	25	2.2×10^{-4}
$[(Ru(bpy)_2)_2BiBzIm]^{2+}$	733	610, 675	60	2.0×10^{-4}
[(bpy)Ru-(BiBzImRu(bpy)$_2$)$_2$]$^{2+}$	734	675	58	2.2×10^{-4}
$[Ru(bpy)_3]^{2+}$[g]	622		620	0.042

[a] In acetonitrile at 298 °C and 4:1 ethanol/methanol glass at 77 K. [b] λ_{ex} = 436 nm. [c] λ_{max}, nm ± 2 nm, corrected. [d] λ_{max}, nm ± 2 nm, uncorrected. [e] τ_0, ±5%. [f] ϕ_r, ±10%. [g] Reference 24.

whether the peak located at 12.2×10^3 cm^{-1} or the shoulder located at 14.2×10^3 cm^{-1} is responsible for the behavior. Further, the bandwidth at half-height, which has been used as a diagnostic test for metal to metal charge transfer, is of little value due to the broad bandwidth associated with the $\pi \rightarrow d\pi$ transition found in the model $[Ru(bpy)_2BiBzImH_2)]^{3+}$ complex. Consequently, little further information can be offered in assigning the origin of the intervalence electron-transfer band of $[Ru^{III}(BiBzIm-Ru^{II}(bpy)_2)_3]^{3+}$. However, qualitatively one notes that the absorption coefficient for $[Ru^{III}(BiBzImRu^{III}(bpy)_2)_3]^{6+}$ is ~3 times greater than for $[Ru^{III}(BiBzImRu^{II}((bpy)_2)_3]^{3+}$, which is in accord with the assignment $\pi \rightarrow d\pi$ (or LMCT).

In summary, the band centered at 12.2×10^3 cm^{-1} displays two types of character. First, it shifts with solvent in a manner characteristic of intervalence electron transfer, and second, it has an intensity and bandwidth in agreement with LMCT character. Thus, the absorption most likely contains overlapping LMCT and M → M charge-transfer bands.

Luminescence. The luminescence properties of the complexes are recorded in Table III. A typical excitation and emission spectrum is illustrated in Figure 9. Emission maxima were located in the 600- and 700-nm region of the spectrum. Low-temperature emission spectra were blue-shifted from room-temperature ones. The monometallic complexes, with the exception of $[Ru(bpy)-(BiBzImH_2)_2]^{2+}$, displayed vibrational structured emission at 77 K; the multimetallic complexes gave only one emission maximum at 77 K. The complexes were weak emitters, as noted from their room-temperature ϕ_r values that ranged from 10^{-3} to 10^{-4}.

The excitation spectra as illustrated in Figure 9 typically displayed the same absorption characteristics as their electronic absorption spectra. The tris chelates, $[Ru(BiImH_2)_3]^{2+}$ and $[Ru(BiBzImH_2)_3]^{2+}$, were nonemitters at both high and low temperature, ruling out involvement of the $BiImH_2$ and $BiBzImH_2$ ligands in the emission decay of the mixed-ligand complexes. Thus,

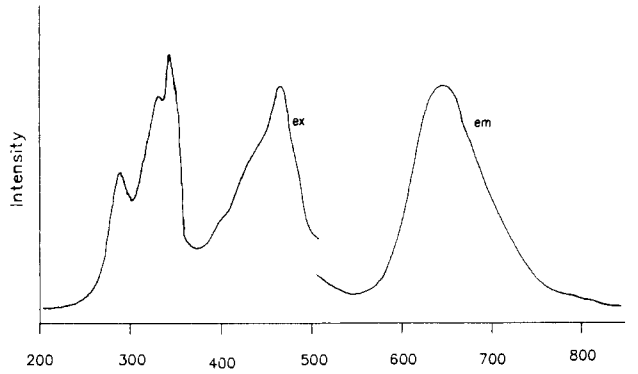

Figure 9. Emission spectrum of $[Ru(bpy)_2(BiBzImH_2)]^{2+}$ exciting at 436 nm and the corresponding excitation spectrum monitoring the emission at 645 nm in acetonitrile at room temperature.

absorption of light most likely populates the ^{3}MLCT state associated with one of the bipyridine ligands and emission is observed from this level analogous to other polypyridyl complexes. In contrast to most multimetallic complexes based on heterocyclic bridging ligands, the bimetallic and trimetallic complexes based on $BiIm^{2-}$ and $BiBzIm^{2-}$ bridging ligands emit due to the fact that the charge transfer occurs to a pendant ligand as opposed to the bridging ligand.

Emission data have previously been reported for $[Ru-(bpy)_2BiImH_2]^{2+}$ and $[Ru(bpy)_2BiBzImH_2]^{2+}$.[21,30] Our results list corrected emission energy maxima for these complexes that are red-shifted from those reported earlier. One notes that the luminescence maxima follow the order $[Ru(bpy)_2(BiImH_2)]^{2+} > [Ru(bpy)(BiImH_2)_2]^{2+} > [(Ru(bpy)_2)_2BiIm]^{2+}$ for the $BiImH_2$ series and $[Ru(bpy)_2(BiBzImH_2)]^{2+} > [Ru(bpy)(BiBzImH_2)_2]^{2+} > [(Ru(bpy)_2)_2BiBzIm]^{2+} > [(bpy)Ru(BiBzImRu(bpy)_2)_2]^{2+}$ for the $BiBzImH_2$ series. Excited-state lifetimes also follow this same trend and vary from approximately 25 to 150 ns with the multimetallic complexes having the shortest lifetimes and the monometallic complexes having the longest lifetimes.

Discussion

Electrostatic Factors. Electrostatic factors have been recognized as important in rationalizing electronic properties of transition-metal complexes.[42] The complexes reported here provide a clearer understanding of their role in altering the redox potential of the $Ru^{3+/2+}$ couple in polypyridyl complexes. Deprotonation of $[Ru(bpy)_2BiBzImH_2]^{2+}$ to give $[Ru(bpy)_2BiBzIm]$ shifts the $Ru^{3+/2+}$ potential from 1.12 to 0.36 V vs SSCE; deprotonation of $[Ru(bpy)(BiBzImH_2)_2]^{2+}$ to give $[Ru(bpy)(BiBzIm)_2]^{2-}$ shifts the $Ru^{3+/2+}$ potential from +0.91 to −0.21 V (see Table II). This effect is electrostatic in nature, leaving a net −2 charge on each BiBzIm ligand. The $d\pi$ orbitals respond to this perturbation by increasing their energy in accord with crystal field theory.[43]

Similar reasoning can be used to account for the redox behavior of multimetallic complexes by considering "$Ru(bpy)_2(L-L)$" as a ligand, where L-L represent a bidentate bridging ligand. Several different forms of $Ru(bpy)_2(L-L)$ have been reported. These are $Ru^{II}(bpy)_2(L-L)$, $Ru^{III}(bpy)_2(L-L)$, and $Ru^{II}(bpy)_2(L-L^{2-})$. If $Ru^{II}(bpy)_2(L-L)$ is used as a frame of reference, $Ru^{III}(bpy)_2(L-L)$ represents a ligand with an additional positive charge; $Ru^{II}-(bpy)_2(L-L^{2-})$ represents a ligand with two additional negative charges. A survey of the literature listing $E_{1/2}(1)$ and $E_{1/2}(2)$ values for the first and second oxidations of $[(bpy)_2Ru(L-L)-Ru(bpy)_2]^{2+}$ complexes,[7,24,25] where L-L is 2,2′-bipyrimidine, 2,3-bis(2-pyridyl)quinoxaline, and 2,3-bis(2-pyridyl)pyrazine, indicates that $E_{1/2}(2)$ increases by 18–20 mV. Thus, addition of two negative charges would be expected to decrease the potential by 36–40 mV. For $[(Ru(bpy)_2)_2BiBzIm]^{2+}$ compared to $[Ru-(bpy)_2BiBzImH_2]^{2+}$, the experimental values for $E_{1/2}(1)$ are 0.76

(42) Callahan, R. W.; Brown, G. M.; Meyer, T. J. *Inorg. Chem.* **1975**, *14*, 1443.
(43) Bethe, J. *Ann. Phys. (Leipzig)* **1929**, *3*, 133. Van Vleck, J. H. *Phys. Rev.* **1932**, *41*, 208. Van Vleck, J. H. *J. Chem. Phys.* **1935**, *3*, 803, 805.

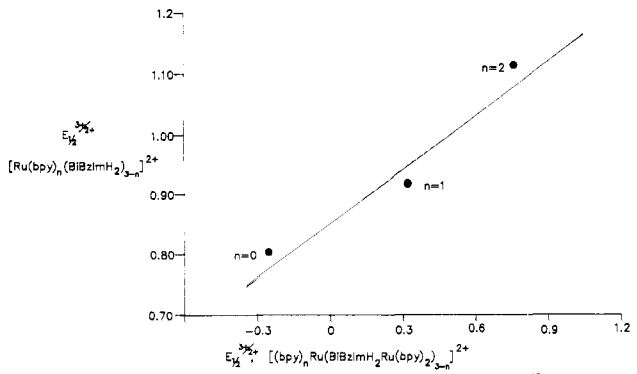

Figure 10. Plot of $E_{1/2}$ for the $[Ru(bpy)_n(BiBzImH_2)_{3-n}]^{3+/2+}$, n = 0–2, series on the vertical axis vs $E_{1/2}$ for the $[Ru(bpy)_n(BiBzImRu(bpy)_2)_{3-n}]^{3+/2+}$, n = 0–2, series on the horizontal axis. The slope is 0.31, and the correlation coefficient is 0.96.

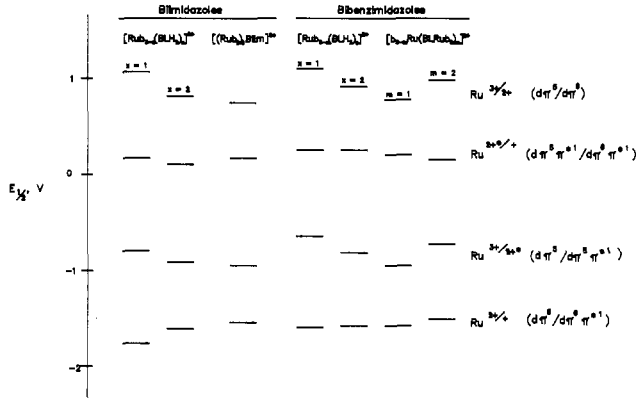

Figure 11. Comparison of ground-state and excited-state redox potentials. The ground-state redox potentials were taken from Table I. The excited-state redox potentials were calculated by the equations given in ref 45.

and 1.12 V, respectively, or a 36-mV change. Similarly, comparing $E_{1/2}(1)$ for $[Ru(BiBzImH_2)_3]^{2+}$ to $E_{1/2}(1)$ for $[Ru(BiBzImRu(bpy)_2)_3]^{2+}$ reveals a 116-mV decrease, which is in the predicted range of a 108–120-mV change. Clearly, the electrostatic factor is dominant in causing the observed $E_{1/2}$ shifts.

Ground-State and Excited-State Redox Properties. As shown in Figure 10, $E_{1/2}$ values for the $[Ru(bpy)_n(BiBzImH_2)_{3-n}]^{2+}$ series correlate with those for the $[Ru(bpy)_n(BiBzImRu(bpy)_2)_{3-n}]^{2+}$ series, n = 0–2. The potentials change over 3 times faster for the multimetallic system than for the monometallic series, which is most likely due to the large increase in electrostatic character associated with the charged bridging ligand(s). Similar correlations were obtained with a ruthenium/rhenium series bridged by 2,2′-bipyrimidine (bpm) for $E_{1/2}'(1)$, where $E_{1/2}'(1)$ was associated with reduction of bpm.[6] In those systems, the multimetallic complexes changed $E_{1/2}'(1)$ values at twice the rate of the monometallic $[Ru(bpy)_n(bpm)_{3-n}]^{2+}$ series, n = 0–2. In contrast, $E_{1/2}'(1)$ values for the bibenzimidazole-based complexes remain relatively fixed due to the fact that bpy is the ligand undergoing reduction, not bibenzimidazole.

Estimates of excited-state redox potentials are given in Figure 11.[44] The excited states are powerful reductants with values comparable to those of $[Ru(bpy)_3]^{2+*}$.[45] As oxidants, however, the excited-state redox potentials are low. The trimetallic complex is of special interest. Excited-state redox potentials can be calculated on the basis of the $Ru^{3+/2+}$ potential for the inner or outer ruthenium unit. However, it is more probable that the origin of the luminescence is from one of the outer "$Ru(bpy)_2$" components rather than the "Ru(bpy)" inner unit. This can be rationalized by noting the similarities in luminescence properties between $[(Ru(bpy)_2)_2BiBIm]^{2+}$ and $[(bpy)Ru(BiBzImRu(bpy)_2)_2]^{2+}$ in Table III. Thus, if $E_{1/2}(2)$ is used as an estimate of the outer $Ru^{3+/2+}$ redox potential, the driving force for the $Ru^{3+/2+*}$ couple would be −0.73 V, which is in the same range as the other complexes in the figure.

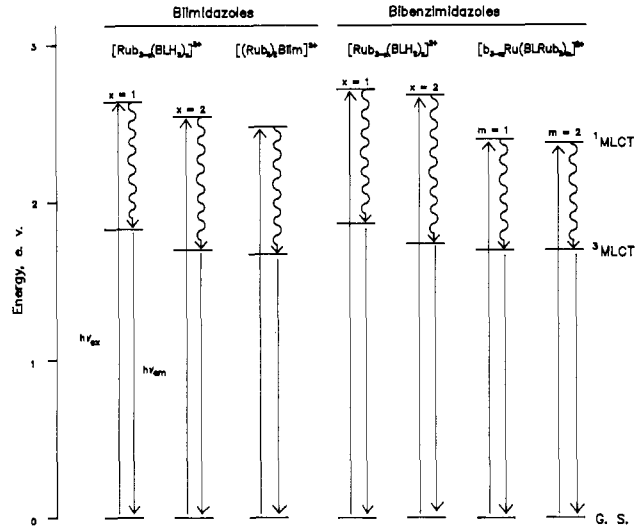

Figure 12. Excited-state energy comparison of the $BiImH_2$-based and $BiBzImH_2$-based complexes. The emission energies fall within the 1.7–1.8-eV range due to the fact that emission occurs from the ^{3}MLCT state associated with the bpy ligand.

The Excited State. Previously, linear correlations between the energy of the ^{1}MLCT transition and the emission energy were reported for ruthenium(II) heterocycles.[7,25] The slopes of these correlations were near 1. The $BiImH_2$ and $BiBzImH_2$ series can be incorporated into these correlations, indicating that their behavior follows that of other ruthenium(II) heterocycles.

A comparison of the excited-state energetics for the $BiImH_2$- and $BiBzImH_2$-based series is given in Figure 12. The emission energies are in the 1.7–1.9-eV range for both series. It is important to note that the multimetallic complexes have emission energies similar to those of the monometallic species. This means the excited-state driving energies are comparable. A further point to note is the possibility of exciting both sides of the bimetallic complex simultaneously e.g. $[(bpy)_2Ru^{II}BiBzImRu^{II}(bpy)_2] \xrightarrow{2h\nu} [(bpy^-)_2Ru^{III}BiBzImRu^{III}(bpy^-)_2]^{2+**}$, resulting in a reagent that can undergo loss of two electrons to a substrate. This idea certainly is plausible given the advent of high-intensity lasers.

Acknowledgment. We thank the Office of Energy Science of the Department of Energy for support under Grant DE-FGO5-84ER-1363. We also thank Johnson-Matthey, Inc., for supplying on loan the $RuCl_3$ used in these studies.

Supplementary Material Available: Table IV, giving elemental analyses of the ruthenium compounds (1 page). Ordering information is given on any current masthead page.

(44) $E_{1/2}(Ru^{3+/2+*}) = E_{1/2}(Ru^{3+/2+}) - E_{em}$; $E_{1/2}(Ru^{2+*/+}) = E_{em} + E_{1/2}(Ru^{2+/+})$.

(45) Sutin, N.; Creutz, C. In *Inorganic and Organometallic Photochemistry*; Wrighton, M. S., Ed.; Advances in Chemistry 168; American Chemical Society: Washington, DC, 1978; pp 1–27.